Cellulose (2020) 27:3277–3286
https://doi.org/10.1007/s10570-019-02962-4

ORIGINAL RESEARCH

Cellulose membranes with polyethylenimine-modified graphene oxide and zinc ions for promoted gas separation

Ting Hou · Lian Shu · Kechun Guo · Xiong-Fei Zhang · Shuai Zhou · Ming He · Jianfeng Yao

Received: 24 July 2019 / Accepted: 26 December 2019 / Published online: 21 January 2020

Abstract Cellulose-based mixed-matrix membranes containing polyethylenimine-modified graphene oxide (PEI-GO) and Zn^{2+} ions were fabricated and used for gas separation. The incorporation of PEI-GO effectively hinders the crystallinity of regenerated cellulose, and PEI-GO was compatible with cellulose matrix and uniformly distributed within the matrix. X-ray photoelectron spectrum revealed the amino group on GO surface can effectively coordinate with Zn^{2+} ions in the membrane. The Zn^{2+} ions content in the membranes increased when increasing the PEI-GO addition. The optimum separation performance was achieved over the membrane with 17 wt‰ PEI-GO (RC-17) wiht the highest zinc content of 24.2 wt%. The corresponding permeability of CO_2 is as high as 268.9 Barrer, and the CO_2/N_2 and CO_2/CH_4 ideal selectivities could reach 48.9 and 57.4, respectively. The enhancement of CO_2 transportation was attributed to both the regulated microstructure of cellulose membrane by PEI-GO and the π-complexation mechanism of Zn^{2+} ions with CO_2 molecules. The prepared membranes would have a highly potential use in the field of CO_2 separation.

Keywords Cellulose membrane · Amino groups · Gas separation · Graphene oxide · Zinc ions · π-complexation

Introduction

Over the past decades, there has been a rising concern on global warming caused by the emission of enormous amounts of CO_2 gases (Adewole et al. 2013; MacDowell et al. 2010). It is extremely urgent to seek a new and efficient separation technology to achieve the collection, purification and reuse of CO_2. Nowadays, gas separation membrane technology shows good prospects in CO_2 capture owing to the advantages of low investment, low energy consumption and easy operation (Olajire 2010; Zhang et al. 2017). Synthetic polymers such as polysulfone, polyethersulfone and polydimethylsiloxane are the mostly applied materials in the fabrication of gas separation membranes. Although they have excellent processing ability, a major limitation is the

Electronic supplementary material The online version of this article (https://doi.org/10.1007/s10570-019-02962-4) contains supplementary material, which is available to authorized users.

T. Hou · K. Guo · S. Zhou · M. He (✉)
College of Science, Nanjing Forestry University, Nanjing 210037, China
e-mail: heming@njfu.edu.cn

L. Shu · X.-F. Zhang · J. Yao (✉)
Jiangsu Co-Innovation Center of Efficient Processing and Utilization of Forest Resources, College of Chemical Engineering, Nanjing Forestry University, Nanjing 210037, China
e-mail: jfyao@njfu.edu.cn

permeability–selectivity trade-off effect (Brunetti et al. 2010). In order to solve this problem, CO_2 transfer-promoting fillers could be introduced into the membrane to simultaneously enhance its permeability and selectivity.

In general, mixed matrix membranes (MMMs) are constructed by loading nanofillers as a dispersed phase into the polymer to form a membrane, which promotes the transport of CO_2 in the polymer membrane (Chung et al. 2013). At present, nanofillers that can construct CO_2 transfer channels mainly include metal-organic frameworks (MOFs), carbon nanotubes (CNTs), graphene oxide (GO), and zeolites, due to their well-defined nanostructure that can serve as high-speed transport channel with high perm-selectivity for gas molecules (Lin et al. 2014; Quan et al. 2017). In our previous work, a composite MOF/cellulose membrane was prepared by wrapping UiO-66-NH_2 (Zr-based MOF) into the densely packed cellulose nanofibrils (CNF-COOH) (Zhang et al. 2018a). The optimum membrane is endowed with enhanced separation performance with CO_2 permeability of 139 Barrer and CO_2/N_2 ideal selectivity of 46. Prior studies proved that GO and its derivatives are ideal inorganic nanofillers for their excellent mechanical properties, atom-thick structure and high aspect ratio (> 1000) (Li et al. 2013, 2015; Wang et al. 2017), which increase the length of the tortuous path of gas diffusion and the selectivity (Zulhairun and Ismail 2014). Zhang et al. (2019) fabricated MMMs by introducing aminosilane functionalized graphene oxide nanosheets (f-GO) into Pebax 1657 matrix. Particularly, Pebax/f-GO-0.9% membrane showed a high CO_2 permeability of 934 Barrer and a CO_2/N_2 selectivity of 41.

Recently, a number of studies have demonstrated that metal ions can act as CO_2 facilitated transport carriers on the basis of π-complexation mechanism, such as Ag^+, Cu^{2+}, Au^+, Co^{2+}, Fe^{2+}, K^+ and Zn^{2+} ions (Ebadi Amooghin et al. 2016; Lee et al. 2012; Liao et al. 2014; Wang et al. 2016a). By the reversible complexation interactions with CO_2, zinc ions can form an unstable Zn–CO_2 complex, so that zinc ions are regarded as good candidate for CO_2 facilitating carrier. Chung and co-workers immobilized zinc ions into polyimide to fabricate composite membrane. The CO_2/CH_4 selectivity of Zn^{2+} ion embedded membrane was 70% greater than that of metal-free membranes (Li and Chung 2008). In our previous work, regenerated cellulose membrane with high zinc ions loading was prepared by dissolving cellulose with $ZnCl_2$ hydrate salts, and exhibited a CO_2 permeability of 155 Barrer with a CO_2/N_2 ideal selectivity of 27 (Zhang et al. 2018b). In Ca–Zn-cellulose system, Zn ions would weaken hydrogen bonds and Ca ions crosslink the Zn-cellulose chains (Sen et al. 2013). However, the CO_2 permeability and separation ratio of the cellulose membrane still have room to improve. The key point is that the cellulose nanofiber membranes obtained *via* physical dissolution and regeneration were densely packed (Wang et al. 2016b; Yang et al. 2011). It is a challenge to simultaneously increase the gas permeate flux and separation ratio of CO_2/N_2.

In this work, we report a facile approach to preparation of mixed matrix membranes by incorporation of PEI-GO and Zn^{2+} ions into cellulose matrix. With the introduction of PEI-GO, the hydrogen bonding network and the crystalline regions of the cellulose were partially destroyed, which increased the length of the tortuous path of gas diffusion and the selectivity. Meanwhile, the content of Zn^{2+} ions, which serve as a fixed carrier to construct a facilitated transport pathway for CO_2, can be regulated by the addition of PEI-GO, taking advantage of the coordination between the grafted amino group and Zn^{2+} ions. To the best of our knowledge, cellulose-based MMMs in this work have the highest permeability and selectivity in terms of CO_2 transport. This strategy could bring new insight in the preparation of gas separation membranes.

Experimental

Materials

In this study, microcrystalline cellulose (DP_v: ∼ 380) and polyethylenimine (PEI, 99%, molecular weight: 10 kDa) were purchased from Aladdin Chemical Reagent Company. $ZnCl_2$ (99%) and $CaCl_2$ (99%) were supplied by Sinopharm Chemical Reagent Company. All chemicals used in this study were of analytical or reagent grade and were used without further purification. Graphene oxide suspension (GO, 2.4 wt%) was bought from the Sixth Element Materials Technology Co., Ltd.

Preparation of PEI-modified GO

Pristine GO was synthesized by the Hummer's method (Hummers and Offeman 1958). Illustration for the preparation of PEI-GO is showed in Scheme 1. In a typical process, 20.8 g of GO suspension (2.4 wt%) was dispersed in 200 mL of deionized water and subjected to ultrasonic treatment for 1 h. Then, the suspension was introduced into a three-necked flask. 1.0 g of PEI was dissolved in 5 mL of deionized water and then added into the above suspension, and the reaction was conducted at 90 °C for 24 h. Subsequently, the obtained suspension was washed by ethanol/water and the water slurry of PEI-GO was formed (Shi et al. 2018). The PEI-GO powder was obtained by centrifugation and the freeze-drying for 24 h.

Preparation of MMMs

Dissolution of cellulose and preparation of membrane were conducted according to the phase-inversion method as described in literatures (Xu et al. 2016; Zhang et al. 2018b). In brief, 9.87 g of $ZnCl_2$ and 0.2 g of $CaCl_2$ were dissolved in deionized water (3.63 g) at 65 °C for 15 min. Simultaneously, 0.45 g of α-cellulose and 1.05 g of deionized water were mixed to obtain cellulose suspension. Then, the $ZnCl_2/CaCl_2$ solution was poured into the cellulose suspension and stirred for another 45 min to obtain cellulose casting solution. Different volume of PEI-GO was added into cellulose casting solution with different filler contents. The solution was degassed under vacuum for 30 min to remove bubbles and cast by a knife (200 μm) over a glass plate. The glass plate was fully immersed into 500 mL of ethanol for 30 min. For convenience of description, the membrane denoted as RC-x and x (= 10, 13, 16, 17, 18 wt‰) refers to the mass percentage of PEI-GO to cellulose. For comparison, pure cellulose membrane, cellulose membrane incorporating by unmodified GO (17 wt‰) as the filler were fabricated following the same method and denoted as RC-0 and RC-GO, respectively.

Characterization of nanofillers and MMMs

Fourier transform infrared (FT-IR) analysis of GO and PEI-GO were obtained by Brucker Vertex-80 V spectrometer. X-ray diffraction (XRD) experiments were conducted by Rigaku Ultima IV with Cu Ka radiation at 40 kV and 30 mA. The elements of nanofillers and the corresponding chemical state were analyzed by X-ray photoelectron spectroscopy (XPS, AXIS UltraDLD). Morphology of the GO and PEI-GO nanosheets were observed by a transmission electron microscope (TEM, JEM-1400, JEOL, Japan). Scanning electron microscopy and X-ray energy

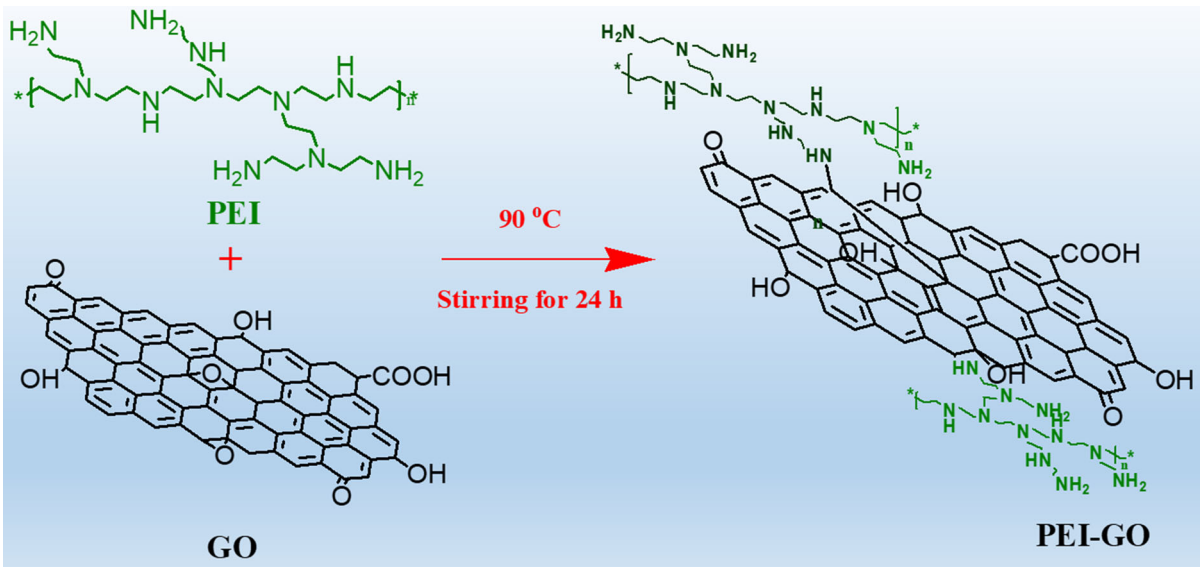

Scheme 1 Reaction mechanism diagram of PEI modified GO.

spectrometer (SEM + EDX, JSM-7600F, JEOL, Japan) were used to explore the morphologies and the distribution of elements of the MMMs.

Gas separation experiments

The gas separation behavior of the MMMs was evaluated from the permeance of single gas. A flat-sheet permeation cell with an effective area of 2.83 cm^2 was used for all tests at room temperature (25 °C) and 0.1 MPa. Before tests, the residual gas in MMMs and pipeline was removed by vacuum pump. The permeability, *Pi* (Barrer) was calculated as Eq. 1 (Xiang et al. 2017a; Xiang et al. 2017b),

$$Pi = \mathrm{NiL}/(\mathrm{A} \cdot \Delta\mathrm{Pi}) \quad (1)$$

where Ni ($cm^3\ s^{-1}$), L (cm), A (cm^2) and ΔPi (cmHg) refer to the volume permeate rate of gas, the film thickness, the test area of membrane, and the pressure drop, respectively.

The ideal selectivity ($S_{i/j}$) was acquired from Eq. 2,

$$S_{i/j} = Pi/Pj \quad (2)$$

where *Pi* and *Pj* correspond to the permeability of single gases of *i* and *j*, respectively.

Results and discussion

Characterization of nanofillers

The functional groups of GO and PEI-GO were investigated by FT-IR. According to Fig. 1a, GO exhibits a prominent peak at around 3300–3400 cm^{-1}, which is assigned to the O–H stretching. The peaks at 1722 and 1060 cm^{-1} are due to the stretching vibration of C=O and the stretching vibration of C–O in epoxy groups, respectively. In addition, the peak at 1223 cm^{-1} corresponds to stretching vibration of C–O in carboxyl groups and the peak at 1610 cm^{-1} is assigned to vibration of C–C. In contrast, it is obvious that PEI-GO shows new peak at 3438 cm^{-1}, which is due to N–H stretching vibration (Shan et al. 2013). Moreover, the intensity of the peak at 1060 cm^{-1} has been remarkably reduced, indicating that epoxy groups of GO had a nucleophilic reaction with the amino groups of PEI. This further demonstrated that PEI molecules are successfully grafted onto the surface of GO nanosheets (Scheme 1). It should be noted that free PEI displays a poor compatibility with membrane matrix and cannot form separation membranes with good uniformity and stability.

The crystalline structures of pristine GO and PEI-GO nanosheets were investigated by XRD (Fig. 1b). The sharp characteristic diffraction peak at 11.6° is ascribed to the (001) plane of GO (Liu et al. 2015). In contrast, the XRD pattern of PEI-GO displays an obvious wide diffraction peak at 21.0°, and the original peak at 11.6° is disappeared, proving that the modified GO was in a disordered state, thereby proving the successful grafting of PEI on GO nanosheets.

PEI-GO illustrates a higher thermal stability than GO and has a mass loss only about 17.8% before 300 °C (Fig. S1, TG details in supporting information). XPS analysis confirm the grafting of PEI on to the surface of GO (Yuan et al. 2016; Zhang et al. 2013). In PEI-GO, the element contents of C, N and O are 66.6%, 20.5% and 12.9%, respectively, successfully endowed GO with PEI functionalization (Fig. S2, XPS in supporting information).

The morphology of GO and PEI-GO was observed by TEM. As shown in Fig. 1c, GO presents multi-layered two-dimensional sheet-like structure with a smooth surface (Zhang et al. 2010). When the GO sheets are grafted with PEI, the sheets of GO are stretched, resulting in the obvious crumpled nanostructure (Fig. 1d). The modification of GO by PEI weakens the agglomeration of GO and enhances the dispersion in the cellulose matrix.

Membrane characterization

The crystallinity changes of the membranes were examined by XRD. From Fig. 2, RC-0 displays peaks at approximately 12.0° and 22.5°, indicating the crystal transformation from cellulose I to cellulose II during the regeneration process (French 2014; Sai et al. 2015). Compared to RC-0, the peak intensity of MMMs are all weakened, which indicates that the incorporation of GO breaks the pristine hydrogen bonding network and destroys the crystalline regions of the cellulose. RC-GO exerts the lowest crystallinity compared with other membranes. With the increase of molecular chain spacing, more transport channels are formed in the membrane, which can facilitate the permeability of gas molecules. TG analyses indicate that the decomposition temperature of the membranes

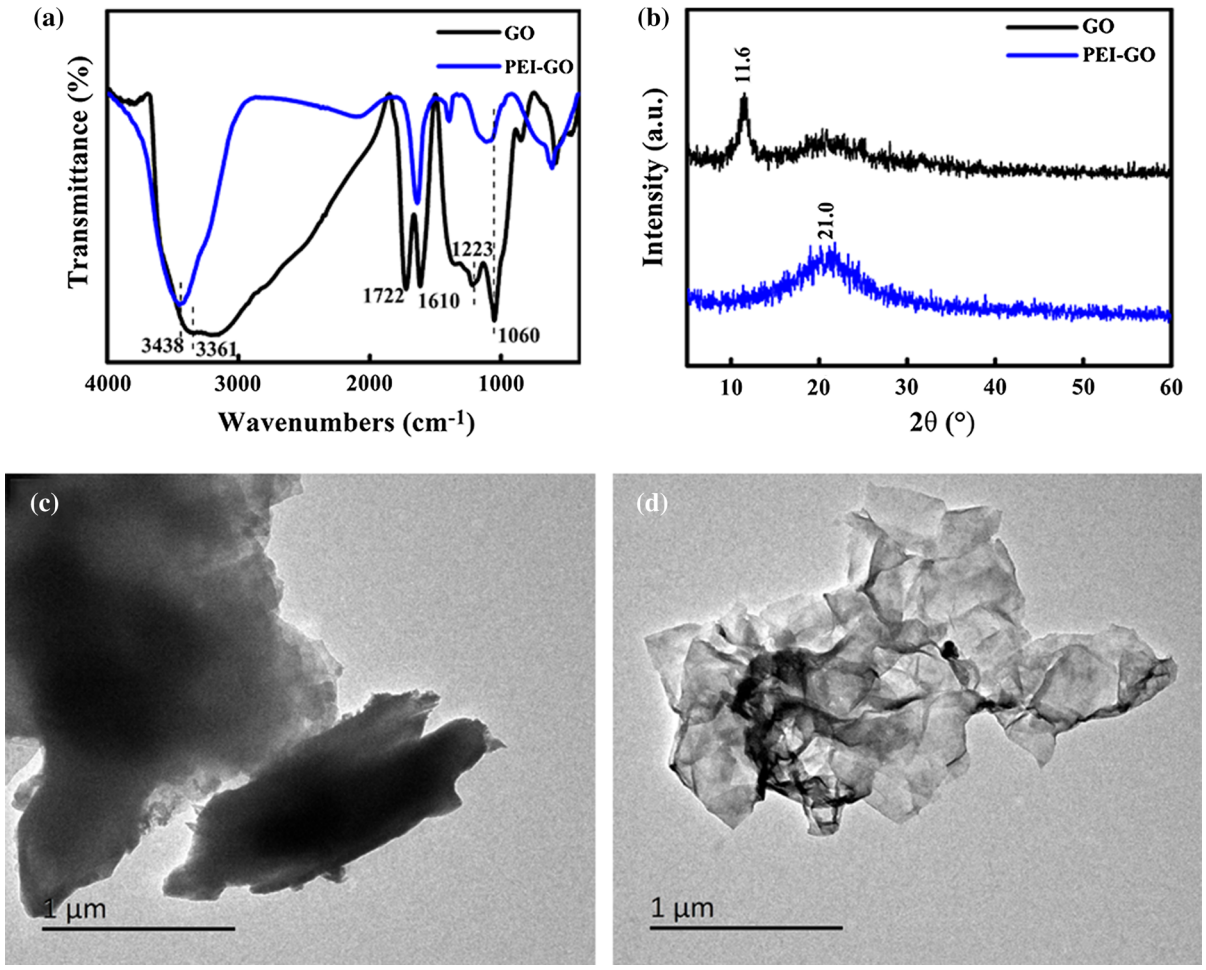

Fig. 1 FT-IR spectra (**a**) and XRD patterns (**b**) of GO and PEI-GO, TEM images of GO (**c**) and PEI-GO (**d**)

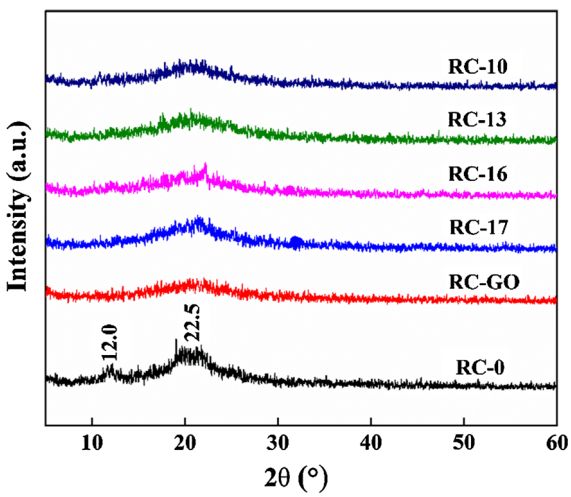

Fig. 2 XRD patterns of the membranes

starts at 213, 229 and 253 °C for RC-0, RC-GO and RC-17, respectively. Among them, RC-17 has a higher decomposition temperature which is attributed to the fact that the modified GO contains a large amount of amino groups that can generate strong hydrogen bonding with hydroxyl of cellulose (Sen et al. 2016). The residual mass of membranes follows the order of RC-17 (49.0%) > RC-GO (42.2%) > RC-0 (27.2%) (details in Fig. S3).

The surface and cross-section morphology of the membranes were examined by SEM. As presented in Fig. 3a, a smooth and homogeneous surface can be observed in RC-0 membrane. With the addition of GO (Fig. 3b), although a few inconspicuous GO particles with size about 1 μm appear on the surface of RC-GO membrane, the membrane still maintains a uniform surface due to the excellent compatibility of GO with

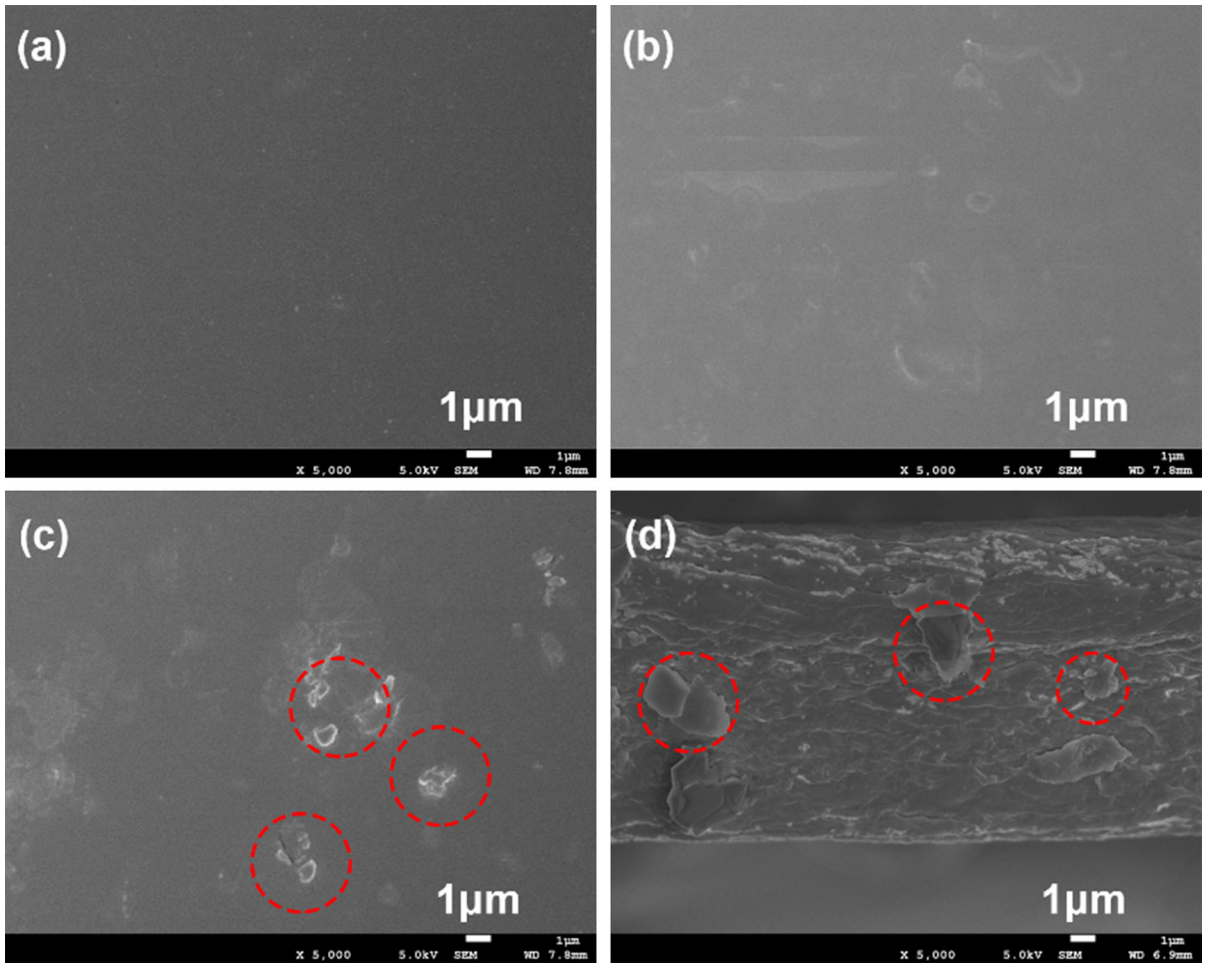

Fig. 3 Surface (**a**–**c**) and cross section (**d**) SEM images of membranes: RC (**a**), RC-GO (**b**) and RC-17 (**c**, **d**), GO-PEI particles shown in red circles

the cellulose. As for RC-17 membrane in Fig. 3c, it can be found that there is no apparent difference with RC-GO membrane. The presence of GO can be observed from the surface and cross-section images of RC-17 membrane (Fig. 3c, d) as designated in red circle.

XPS measurement was used to further provide more details about the elemental composition and chemical bonds of RC-17. Figure 4a shows that Zn element is successfully loaded into the MMMs. To ascertain the Zn^{2+} coordination bonds, the XPS spectrum of Zn 2p is divided into two peaks by Origin software. As presented in Fig. 4b, two peaks centered at 1022.64 and 1023.06 eV can be assigned to Zn–O and Zn–N bonds, respectively (Liu et al. 2016), suggesting the coordination of Zn^{2+} and PEI-GO nanosheets.

Gas separation tests

Gas permeation over different MMMs was tested by a feed pressure of 0.1 MPa and 25 °C. The pristine RC-0 membrane has a CO_2 permeability of 26.0 Barrer. In terms of RC-GO membrane, the CO_2 permeability is 127.6 Barrer. The improvement of gas permeability is attributed to the incorporation of GO in the matrix (Table S1). The GO sheet structure with high-aspect ratio leads to the highly tortuous diffusion path in the cellulose matrix and generates a rigidified interface between cellulose matrix and fillers (Jia et al. 2019), leading to a significant improvement the CO_2/N_2 selectivity of RC-GO membrane.

With the introduction of PEI-GO, the MMMs show a higher permeability and selectivity to CO_2, while

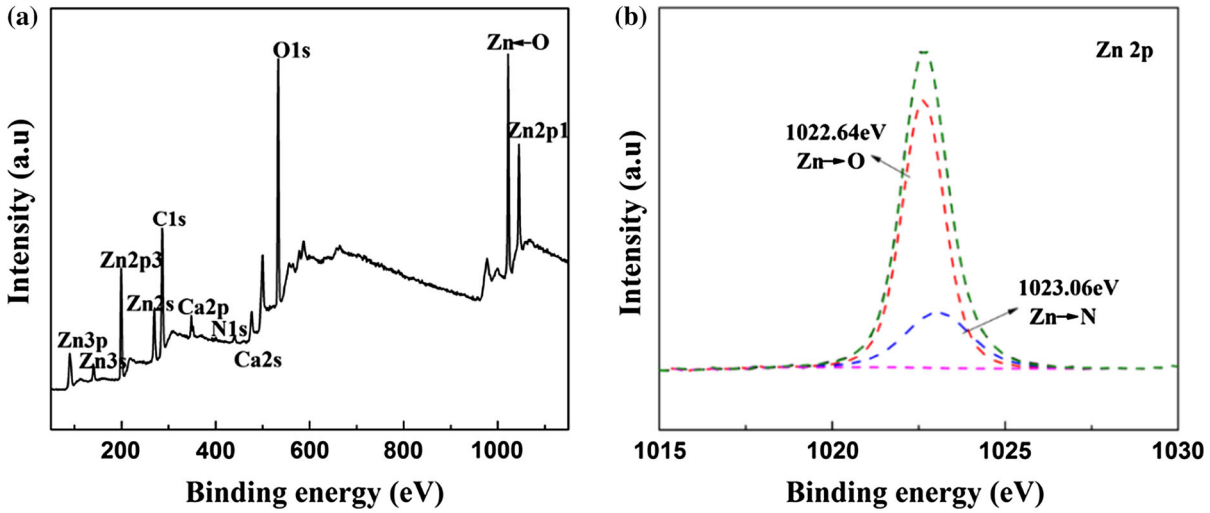

Fig. 4 XPS spectrum (**a**) and Zn 2p spectrum (**b**) of RC-17

there is no significant change of the permeability of N_2 and CH_4 except for RC-18 membrane (Fig. 5). It can be observed that the CO_2 permeability and CO_2/N_2 selectivity increase substantially with the increase of PEI-GO content. The membrane containing 17 wt‰ PEI-GO exhibits an optimal separation performance with a CO_2 permeability of 268.9 Barrer and a CO_2/N_2 ideal selectivity of 48.9 (Fig. 5a). The same tendency was observed for CO_2/CH_4. As shown in Fig. 5b, CH_4 exhibits lower permeabilities due to the large kinetic diameter of CH_4 (3.8 Å). However, when the PEI-GO content increases to 18 wt%, both CO_2/N_2 and CO_2/CH_4 selectivities were sharply decreased (more PEI-GO loadings can be found in Table S1), which should relate to the presence of interfacial defects. Such defects were caused by the excess amount of PEI-GO, which formed agglomerates and reduced the uniformity of as-prepared membranes. The pressure effects were investigated by elevating the feeding pressure from 0.1 to 0.4 MPa. The permeability of CO_2 for RC-17 increases (Table S2), which is ascribed to interaction between CO_2 molecules and zinc ions located on cellulose chains.

In order to explore the effect of amino on Zn^{2+} ions loading capacity in MMMs, energy-dispersive X-ray (EDX) analysis was recorded. The results shows that Zn^{2+} ions content is significantly increased by 83% from 13.2 to 24.2 wt% with the increase of PEI-GO

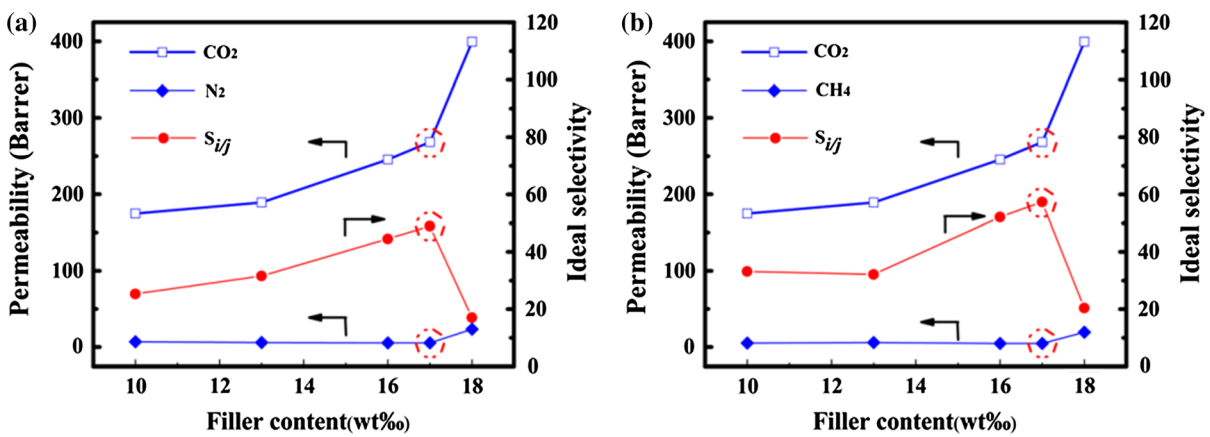

Fig. 5 Permeability and selectivity over mixed-matrix membranes with PEI-GO, gas separation performance of CO_2/N_2 (**a**) and CO_2/CH_4 (**b**)

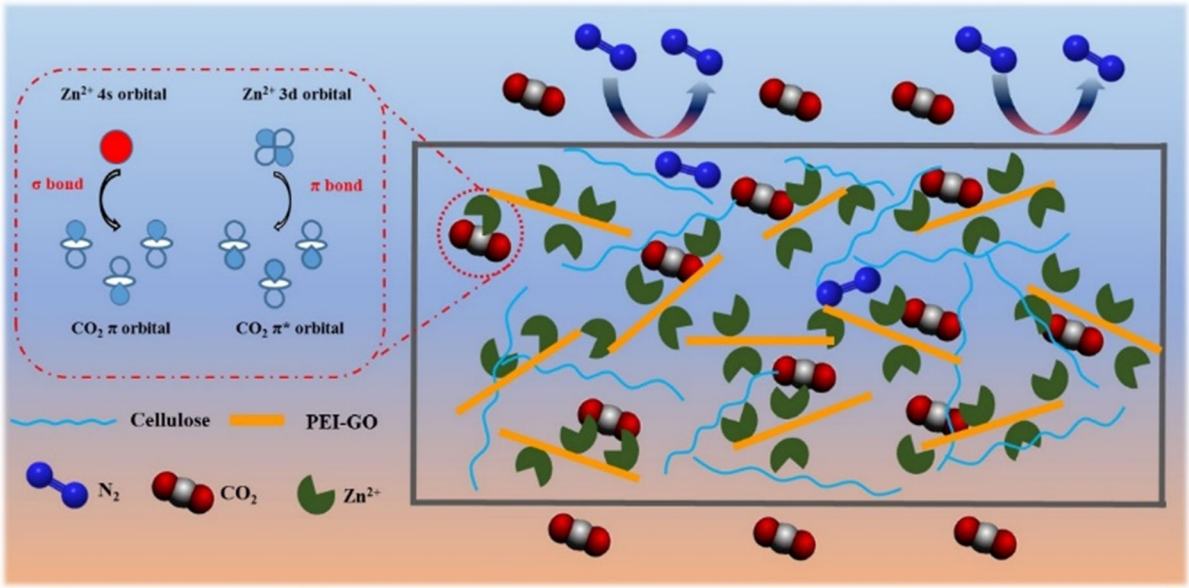

Fig. 6 Mechanism illustration of CO_2 transport with high permeability and selectivity

loading from 10 (RC-10) to 17 wt% (RC-17). This is sufficient to verify that the increase of amino group can effectively carry more Zn^{2+} ions, thus effectively promote the CO_2 permeability (details summarized in Table S3). More Zn^{2+} ions in the membranes will provide more transport carrier to CO_2 via a π-complexation mechanism, as depicted in Fig. 6 (Peng et al. 2017). In addition, it should be mentioned that –NH_2 groups may provide effective CO_2 adsorption site and increase the affinity toward CO_2 (Wu et al. 2014). Amino groups would act as non-ionic CO_2 carriers through covalent connection to cellulose chains and facilitate CO_2 transport. Nevertheless, due to the small change of N contents (Table S3), the impact on CO_2 permeability should be negligible. It is proposed that PEI-GO nanofillers not only construct more tortuous gas diffusion path, but also provide effective transport carrier to CO_2. The designed RC-17 membrane breaks the trade-off relationship between permeability and selectivity due to the synergistic effect of Zn^{2+} ions and PEI-GO.

Conclusion

In this work, a novel facilitated transport membrane for effective CO_2/N_2 separation was successfully fabricated by incorporating PEI-modified GO nanofiller into regenerated cellulose membranes. The enhanced CO_2 transport through membrane is attributed to the synergistic effect of Zn^{2+} ions and PEI-GO. The incorporation of PEI-GO breaks the pristine hydrogen bonding networks and destroys the crystalline regions of the cellulose. The abundant –NH_2 groups over PEI could interact with the hydroxyl groups over cellulose, giving to a good dispersion of fillers in the membrane matrix. High Zn^{2+} ions loading on membranes was achieved *via* the coordination with –NH_2 functional groups. The CO_2 permeability increased substantially with the increase of PEI-GO content. However, the maximum of CO_2/N_2 separation ratio was achieved when the PEI-GO content was at 17‰. The optimum cellulose membrane exhibited an excellent CO_2 permeability of 268.9 Barrer with a high CO_2/N_2 ideal selectivity of 48.9, breaking through the permeability-selectivity trade-off. This innovative preparation strategy makes it possible to use regenerated cellulose membranes on a large scale for gas separation.

Acknowledgments The authors are grateful for financial supports from the Priority Academic Program Development of Jiangsu Higher Education Institutions (PAPD). The authors also thank the testing services from Advanced Analysis & Testing Center of Nanjing Forestry University.

References

Adewole JK, Ahmad AL, Ismail S, Leo CP (2013) Current challenges in membrane separation of CO_2 from natural gas: a review. Int J Greenh Gas Control 17:46–65

Brunetti A, Scura F, Barbieri G, Drioli E (2010) Membrane technologies for CO_2 separation. J Membr Sci 359:115–125

Chung Y-L, Olsson JV, Li RJ, Frank CW, Waymouth RM, Billington SL, Sattely ES (2013) A renewable Lignin–Lactide copolymer and application in biobased composites. ACS Sustain Chem Eng 1:1231–1238

Ebadi Amooghin A, Omidkhah M, Sanaeepur H, Kargari A (2016) Preparation and characterization of Ag^+ ion-exchanged zeolite-Matrimid®5218 mixed matrix membrane for CO_2/CH_4 separation. J Energy Chem 25:450–462

French AD (2014) Idealized powder diffraction patterns for cellulose polymorphs. Cellulose 21:885–896

Hummers WS, Offeman RE (1958) Preparation of Graphitic Oxide. J Am Chem Soc 80:1339–1339

Jia M, Feng Y, Qiu J, Zhang X-F, Yao J (2019) Amine-functionalized MOFs@GO as filler in mixed matrix membrane for selective CO_2 separation. Sep Purif Technol 213:63–69

Lee JH, Hong J, Kim JH, Kang YS, Kang SW (2012) Facilitated CO_2 transport membranes utilizing positively polarized copper nanoparticles. Chem Commun 48:5298–5300

Li H, Song ZN, Zhang XJ, Huang Y, Li SG, Mao YT, Ploehn HJ, Bao Y, Yu M (2013) Ultrathin, molecular-sieving graphene oxide membranes for selective hydrogen separation. Science 342:95–98

Li Y, Chung TS (2008) Highly selective sulfonated polyethersulfone (SPES)-based membranes with transition metal counterions for hydrogen recovery and natural gas separation. J Membr Sci 308:128–135

Li Y, Wang S, He G, Wu H, Pan F, Jiang Z (2015) Facilitated transport of small molecules and ions for energy-efficient membranes. Chem Soc Rev 44:103–118

Liao J, Wang Z, Gao C, Li S, Qiao Z, Wang M, Zhao S, Xie X, Wang J, Wang S (2014) Fabrication of high-performance facilitated transport membranes for CO_2 separation. Chem Sci 5:2843–2849

Lin R, Ge L, Hou L, Strounina E, Rudolph V, Zhu Z (2014) Mixed matrix membranes with strengthened MOFs/polymer interfacial interaction and improved membrane performance. ACS Appl Mater Interfaces 6:5609–5618

Liu J, Liu Z, Barrow CJ, Yang W (2015) Molecularly engineered graphene surfaces for sensing applications: a review. Anal Chim Acta 859:1–19

Liu L, Huang G, Song P, Yu Y, Fu S (2016) Converting industrial alkali lignin to biobased functional additives for improving fire behavior and smoke suppression of polybutylene succinate. ACS Sustain Chem Eng 4:4732–4742

MacDowell N, Florin N, Buchard A, Hallett J, Galindo A, Jackson G, Adjiman CS, Williams CK, Shah N, Fennell P (2010) An overview of CO_2 capture technologies. Energy Environ Sci 3:426–443

Olajire AA (2010) CO_2 capture and separation technologies for end-of-pipe applications: a review. Energy 35:2610–2628

Peng D, Wang S, Tian Z, Wu X, Wu Y, Wu H, Xin Q, Chen J, Cao X, Jiang Z (2017) Facilitated transport membranes by incorporating graphene nanosheets with high zinc ion loading for enhanced CO_2 separation. J Membr Sci 522:351–362

Quan S, Li SW, Xiao YC, Shao L (2017) CO_2-selective mixed matrix membranes (MMMs) containing graphene oxide (GO) for enhancing sustainable CO_2 capture. Int J Greenh Gas Control 56:22–29

Sai H, Fu R, Xing L, Xiang J, Li Z, Li F, Zhang T (2015) Surface modification of bacterial cellulose aerogels' web-like skeleton for oil/water separation. ACS Appl Mater Interfaces 7:7373–7381

Sen S, Martin JD, Argyropoulos DS (2013) Review of cellulose non-derivatizing solvent interactions with emphasis on activity in inorganic molten salt hydrates, ACS Sustain. Chem Eng 1:858–870

Sen S, Losey BP, Gordon EE, Argyropoulos DS, Martin JD (2016) Ionic liquid character of zinc chloride hydrates define solvent characteristics that afford the solubility of cellulose. J Phys Chem B 120:1134–1141

Shan C, Wang L, Han D, Li F, Zhang Q, Zhang X, Niu L (2013) Polyethyleneimine-functionalized graphene and its layer-by-layer assembly with Prussian blue. Thin Solid Films 534:572–576

Shi Y, Yu B, Zheng Y, Yang J, Duan Z, Hu Y (2018) Design of reduced graphene oxide decorated with DOPO-phosphanomidate for enhanced fire safety of epoxy resin. J Colloid Interface Sci 521:160–171

Wang S, Liu Y, Zhang M, Shi D, Li Y, Peng D, He G, Wu H, Chen J, Jiang Z (2016a) Comparison of facilitated transport behavior and separation properties of membranes with imidazole groups and zinc ions as CO_2 carriers. J Membr Sci 505:44–52

Wang S, Lu A, Zhang L (2016b) Recent advances in regenerated cellulose materials. Prog Polym Sci 53:169–206

Wang S, Xie Y, He G, Xin Q, Zhang J, Yang L, Li Y, Wu H, Zhang Y, Guiver MD, Jiang Z (2017) Graphene oxide membranes with heterogeneous nanodomains for efficient CO_2 separations. Angew Chem Int Ed 56:14246–14251

Wu H, Li X, Li Y, Wang S, Guo R, Jiang Z, Wu C, Xin Q, Lu X (2014) Facilitated transport mixed matrix membranes incorporated with amine functionalized MCM-41 for enhanced gas separation properties. J Membr Sci 465:78–90

Xiang L, Pan Y, Jiang J, Chen Y, Chen J, Zhang L, Wang C (2017a) Thin poly(ether-block-amide)/attapulgite composite membranes with improved CO_2 permeance and selectivity for CO_2 /N_2 and CO_2 /CH_4 Chem Eng Sci 160:236–244

Xiang L, Sheng L, Wang C, Zhang L, Pan Y, Li Y (2017b) Amino-functionalized ZIF-7 nanocrystals: improved intrinsic separation ability and interfacial compatibility in mixed-matrix membranes for CO_2 /CH_4 separation. Adv Mater 29:1606999

Xu Q, Chen C, Rosswurm K, Yao T, Janaswamy S (2016) A facile route to prepare cellulose-based films. Carbohydr Polym 149:274–281

Yang Q, Fukuzumi H, Saito T, Isogai A, Zhang L (2011) Transparent cellulose films with high gas barrier properties fabricated from aqueous alkali/urea solutions. Biomacromol 12:2766–2771

Yuan B, Xing W, Hu Y, Mu X, Wang J, Tai Q, Li G, Liu L, Liew KM, Hu Y (2016) Boron/phosphorus doping for retarding the oxidation of reduced graphene oxide. Carbon 101:152–158

Zhang C, Hao R, Liao H, Hou Y (2013) Synthesis of amino-functionalized graphene as metal-free catalyst and exploration of the roles of various nitrogen states in oxygen reduction reaction. Nano Energy 2:88–97

Zhang J, Yang H, Shen G, Cheng P, Zhang J, Guo S (2010) Reduction of graphene oxide via L-ascorbic acid. Chem Commun 46:1112–1114

Zhang J, Xin Q, Li X, Yun M, Xu R, Wang S, Li Y, Lin L, Ding X, Ye H, Zhang Y (2019) Mixed matrix membranes comprising aminosilane-functionalized graphene oxide for enhanced CO_2 separation. J Membr Sci 570–571:343–354

Zhang XF, Feng Y, Huang C, Pan Y, Yao J (2017) Temperature-induced formation of cellulose nanofiber film with remarkably high gas separation performance. Cellulose 24:5649–5656

Zhang XF, Feng Y, Wang Z, Jia M, Yao J (2018a) Fabrication of cellulose nanofibrils/UiO-66-NH_2 composite membrane for CO_2/N_2 separation. J Membr Sci 568:10–16

Zhang XF, Hou T, Chen J, Feng Y, Li B, Gu X, He M, Yao J (2018b) Facilitated transport of CO_2 through the transparent and flexible cellulose membrane promoted by fixed-site carrier. ACS Appl Mater Interfaces 10:24930–24936

Zulhairun AK, Ismail AF (2014) The role of layered silicate loadings and their dispersion states on the gas separation performance of mixed matrix membrane. J Membr Sci 468:20–30